Enhancement of fluorescence emission and signal gain at 1.53 μm in Er^{3+}/Ce^{3+} co-doped tellurite glass fiber*

YANG Feng-jing (杨风景)**, **HUANG Bo** (黄波), **WU Li-bo** (吴立波), **QI Ya-wei** (齐亚伟), **PENG Sheng-xi** (彭胜喜), **LI Jun** (李军), **and ZHOU Ya-xun** (周亚训)

College of Information Science and Engineering, Ningbo University, Ningbo 315211, China

(Received 18 June 2015)

Er^{3+}/Ce^{3+} co-doped tellurite glasses with composition of TeO_2-GeO_2-Li_2O-Nb_2O_5 were prepared using conventional melt-quenching technique for potential applications in Er^{3+}-doped fiber amplifier (EDFA). The absorption spectra, up-conversion spectra and 1.53 μm band fluorescence spectra of glass samples were measured. It is shown that the 1.53 μm band fluorescence emission intensity of Er^{3+}-doped tellurite glass fiber is improved obviously with the introduction of an appropriate amount of Ce^{3+}, which is attributed to the energy transfer (ET) from Er^{3+} to Ce^{3+}. Meanwhile, the 1.53 μm band optical signal amplification is simulated based on the rate and power propagation equations, and an increment in signal gain of about 2.4 dB at 1 532 nm in the Er^{3+}/Ce^{3+} co-doped tellurite glass fiber is found. The maximum signal gain reaches 29.3 dB on a 50 cm-long fiber pumped at 980 nm with power of 100 mW. The results indicate that the prepared Er^{3+}/Ce^{3+} co-doped tellurite glass is a good gain medium applied for 1.53 μm broadband and high-gain EDFA.

Document code: A **Article ID:** 1673-1905(2015)05-0361-5

DOI 10.1007/s11801-015-5111-1

In recent years, the optical amplifier with a wide and flat gain spectrum is urgently needed for the wavelength-division-multiplexing (WDM) communication systems[1]. Er^{3+}-doped fiber amplifier (EDFA) with a flat gain spectrum across both C-band and L-band has been demonstrated in tellurite-based glasses[2]. Tellurite glass has many excellent characteristics, such as easier preparation, better physical stability and chemical durability, larger transparency window (0.35–5.00 μm), higher rare-earth (RE) ion solubility, higher refractive index (~2.0) and lower phonon energy (~750 cm^{-1})[3,4], which make it a promising candidate for the development of broadband EDFA and other photonic devices.

In order to obtain a good noise figure, the 980 nm pumping scheme is usually adopted for EDFA operating in the 1.53 μm band[5]. However, due to the low phonon energy of tellurite glass (~750 cm^{-1}), the strong visible band up-conversion emission caused by the excited state absorption (ESA) in Er^{3+} doped tellurite glasses under the 980 nm excitation decreases the efficiency of 1.53 μm band fluorescence emission[6,7]. Er^{3+}/Ce^{3+} co-doping is an effective method to suppress the visible band up-conversion emission through the energy transfer (ET) process of Er^{3+}:$^4I_{11/2}$+Ce^{3+}:$^2F_{5/2}$→Er^{3+}:$^4I_{13/2}$+Ce^{3+}:$^2F_{7/2}$[8]. In this paper, Er^{3+}/Ce^{3+} co-doped tellurite glass with composition of TeO_2-GeO_2-Li_2O-Nb_2O_5 was prepared to explore the feasibility of improving the 1.53 μm band fluorescence emission of Er^{3+} and the 1.53 μm band signal gain with the help of the ET from Er^{3+} to Ce^{3+} under the 980 nm excitation.

The Er^{3+}/Ce^{3+} co-doped tellurite glass samples with molar compositions of $(74-x)TeO_2$-$15GeO_2$-$5Li_2O$-$5Nb_2O_5$-$1Er_2O_3$-xCe_2O_3 were prepared in alumina crucibles at 950 °C for about 30 min, in which x=0, 0.5, 1 and 2, labeled as TEC0, TEC1, TEC2 and TEC3, respectively. The obtained high temperature glass melt was casted immediately into a preheated stainless steel mold, then annealed at 10 °C below the glass transition temperature for 2 h, and finally cooled down to the room temperature slowly. All the glass samples were cut and polished into the same size of 10 mm×10 mm×2 mm to meet the requirements for further spectroscopic measurement.

The glass sample density was obtained based on the Archimede principle using distilled water as an immersion liquid. The refractive index was measured with a prism coupler at 632.8 nm. The doped RE ion concentrations were calculated from the measured sample density and the initial composition, and the obtained results are listed in Tab.1. The ultraviolet / visible/near infrared (UV/Vis/NIR) absorption spectra of glass samples in the wavelength range of 400–1 600 nm were recorded with a Perkin-Elmer-Lambda 950 spectra photometer. The

* This work has been supported by the National Natural Science Foundation of China (No.61177087), the Graduate Innovative Scientific Research Project of Zhejiang Province (No.YK2010048), the Scientific Research Foundation of Graduate School of Ningbo University (No.G13035), and K. C. Wong Magna Fund and Hu Lan Outstanding Doctoral Fund in Ningbo University.

** E-mail:fengjfengm@163.com

fluorescence emission spectra were measured with a Jobin Yvon Triax550 spectrophotometer under excitation of a 975 nm LD with a maximum power of 2 W. These above measurements were performed at room temperature.

Tab.1 Density ρ, refractive index n, Er^{3+} and Ce^{3+} concentrations N_{Er} and N_{Ce}, fluorescence lifetime τ_m, spontaneous radiative transition probability A_{rad}, radiative lifetime τ_{rad} and branching radio β in TEC0 and TEC2 glass samples

Parameter		Value (TEC0)	Value (TEC2)
ρ (g/cm^3)		4.930	4.950
n		2.010	2.019
N_{Er} ($\times10^{20}$ cm^{-3})		3.806	3.782
N_{Ce} ($\times10^{20}$ cm^{-3})		0	3.782
$^4I_{13/2}\rightarrow{}^4I_{15/2}$	τ_m (ms)	3.25	3.09
$^4I_{13/2}\rightarrow{}^4I_{15/2}$	A_{rad} (s^{-1})	297.73	313.82
	τ_{rad} (ms)	3.36	3.19
$^4I_{11/2}\rightarrow{}^4I_{13/2}$	A_{rad} (s^{-1})	57.50	57.26
$^4I_{11/2}\rightarrow{}^4I_{15/2}$	A_{rad} (s^{-1})	280.75	279.57
$^4I_{11/2}\rightarrow{}^4I_{13/2}+{}^4I_{15/2}$	A_{rad} (s^{-1})	338.25	336.83
	τ_{rad} (ms)	2.96	2.97
$^4I_{13/2}\rightarrow{}^4I_{15/2}$	β	1	
$^4I_{11/2}\rightarrow{}^4I_{15/2}$	β	0.83	0.83
$^4I_{11/2}\rightarrow{}^4I_{13/2}$	β	0.17	0.17

The energy level diagram of Er^{3+} and Ce^{3+} pumped at 980 nm is shown in Fig.1.

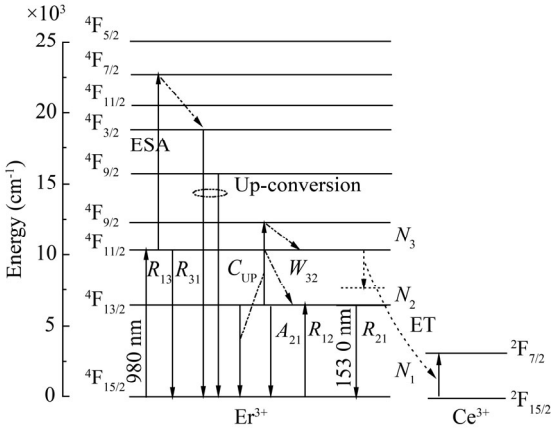

Fig.1 The energy level diagram of Er^{3+} and Ce^{3+} pumped at 980 nm

Fig.2 shows the measured absorption spectra of Er^{3+} single-doped TEC0 and Er^{3+}/Ce^{3+} co-doped TEC1–TEC3 glass samples in the wavelength range from 400 nm to 1 600 nm. The absorption spectrum of TEC0 glass sample contains eight absorption peaks centered at 452 nm, 488 nm, 521 nm, 545 nm, 652 nm, 800 nm, 975 nm and 1 530 nm, which are assigned to the transitions from the ground state $^4I_{15/2}$ to the different excited levels of $^4F_{5/2}$, $^4F_{7/2}$, $^2H_{11/2}$, $^4S_{3/2}$, $^4F_{9/2}$, $^4I_{9/2}$, $^4I_{11/2}$ and $^4I_{13/2}$ of Er^{3+}, respectively, whereas the absorption bands below 500 nm are obscured in the TEC1–TEC3 glass samples due to the strong absorption resulting from the inter-configurational transition ($4f^1\rightarrow4f^0,5d^1$) of Ce^{3+}[9]. According to the Judd-Ofelt theory[10,11], some important spectroscopic parameters of Er^{3+}, such as the radiative transition probability A_{rad}, radiative lifetime τ_{rad} and fluorescence branching ratio β, can be calculated from the absorption spectrum, and the obtained results of TEC0 and TEC2 glass samples are listed in Tab.1. The radiative transition probability of Er^{3+}:$^4I_{13/}\rightarrow{}^4I_{15/2}$ transition is calculated to be 313.82 s^{-1} in the TEC2 glass sample, which is larger than that in the TEC0 glass sample. The large transition probability is beneficial for achieving intense 1.53 μm fluorescence emission.

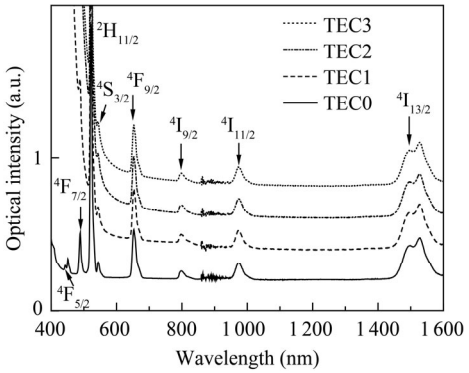

Fig.2 Absorption spectra of TEC0–TEC3 glass samples

Fig.3 displays the measured 1.53 μm band fluorescence spectra corresponding to Er^{3+}:$^4I_{13/2}\rightarrow{}^4I_{15/2}$ transition of TEC0–TEC3 glass samples under the 975 nm excitation. The inset shows the fluorescence integrated intensities of TEC0–TEC3 glass samples. It is seen that the prepared Er^{3+}-doped tellurite glasses exhibit similar broad fluorescence emissions (ranging from 1 450 nm to 1 650 nm), and the obtained full width at half maximum (*FWHM*) values in Er^{3+} single-doped TEC0 glass sample and Er^{3+}/Ce^{3+} co-doped TEC2 glass sample are 65 nm and 70 nm, respectively. Compared with the TEC0 glass sample, however, the fluorescence intensities of TEC1 and TEC2 glass samples increase obviously with the addition of Ce^{3+}, which can be attributed to the ET between Er^{3+}:$^4I_{11/2}$ level and Ce^{3+}:$^2F_{7/2}$ level, as depicted in Fig.1. Through this ET process, excited Er^{3+} ions at the pumping $^4I_{11/2}$ level transfer their energy to Ce^{3+} ions at ground state, and return rapidly to the fluorescence emitting level $^4I_{13/2}$, therefore, the 1.53 μm band fluorescence intensity increases accordingly. However, when the Ce^{3+} concentration is larger than 1%, the fluorescence intensity tends to decrease, and the reason may be that the larger Ce^{3+} concentration results in the backward ET from Ce^{3+} to Er^{3+}. Therefore, there is an appropriate doping concentration for Er^{3+}/Ce^{3+} co-doping scheme.

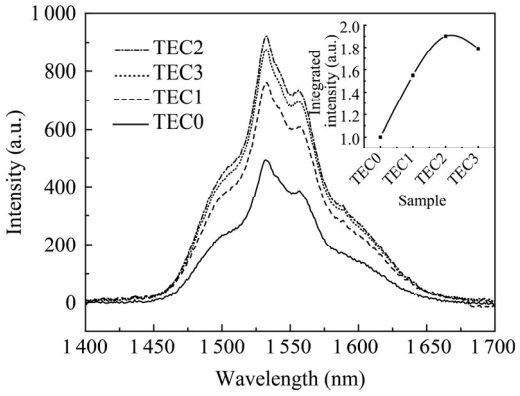

Fig.3 Fluorescence spectra of TEC0–TEC3 glass samples (The inset descripts fluorescence integrated intensities of TEC0–TEC3 glass samples.)

Fig.4 displays the measured visible band up-conversion emission spectra in the wavelength range of 400–700 nm for Er^{3+} single-doped TEC0 and Er^{3+}/Ce^{3+} co-doped TEC1–TEC3 glass samples under the 975 nm excitation. The observed strong green emissions centered at 527 nm and 550 nm and the red emission centered at 662 nm in the TEC0 glass sample are assigned to $^2H_{11/2}\rightarrow{}^4I_{15/2}$, $^4S_{3/2}\rightarrow{}^4I_{15/2}$ and $^4F_{9/2}\rightarrow{}^4I_{15/2}$ transitions of Er^{3+}, respectively[12,13]. As expected, with the introduction of Ce^{3+}, the up-conversion emission decreases dramatically, which is attributed to the ET from Er^{3+}:$^4I_{11/2}$ to Ce^{3+}:$^2F_{7/2}$ level as discussed above, and finally it leads to the depopulation of Er^{3+} at $^4I_{11/2}$ level.

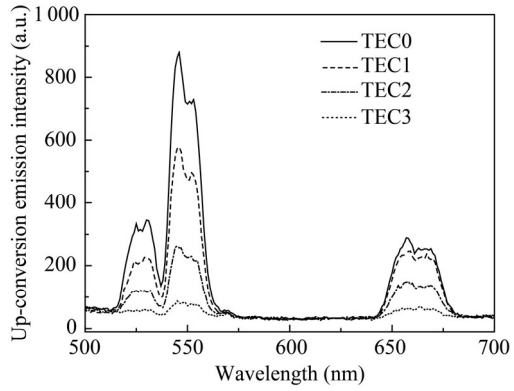

Fig.4 Up-conversion spectra of TEC0–TEC3 glass samples under 975 nm excitation

It is clear that Er^{3+}/Ce^{3+} co-doping can evidently enhance the 1.53 μm band fluorescence through suppressing the visible band up-conversion emission under the 980 nm excitation. In order to reveal the feasibility of Er^{3+}/Ce^{3+} co-doped tellurite glass as a gain medium for broadband EDFA and understand the effect of ET on the improvement of 1.53 μm band signal gain, the optical signal amplification of Er^{3+}/Ce^{3+} co-doped tellurite glass fiber is investigated theoretically. The 1.53 μm band optical signal amplification can be regarded approximately as a three-level system under the 980 nm excitation. Er^{3+} ions are first excited from the ground state $^4I_{15/2}$ to the pumping level $^4I_{11/2}$ via ground state absorption (GSA) of pump photons, and then rapidly relax to the fluorescence emitting level $^4I_{13/2}$ through combining ET process from Er^{3+} to Ce^{3+} and multiphonon relaxation process. The 1.53 μm band signal amplification occurs with Er^{3+} being stimulated by the input signal photons when the population inverts between $^4I_{13/2}$ and $^4I_{15/2}$ levels. For the sake of simplicity, two assumptions are made here: all the Er^{3+} ions excited to the $^4I_{9/2}$ level by the cooperative up-conversion process of $^4I_{13/2}+{}^4I_{13/2}\rightarrow{}^4I_{9/2}+{}^4I_{15/2}$ relax immediately to the $^4I_{11/2}$ level, and the ESA of Er^{3+} ions at the $^4I_{11/2}$ level is neglected. Thus, the variations of Er^{3+} populations with time at levels $^4I_{15/2}$, $^4I_{13/2}$ and $^4I_{11/2}$ can be expressed as[2]

$$\frac{\mathrm{d}N_1}{\mathrm{d}t}=-(R_{13}+R_{12})N_1+(A_{21}+R_{21})N_2+C_{up}N_2^2+R_{31}N_3, \tag{1}$$

$$\frac{\mathrm{d}N_2}{\mathrm{d}t}=R_{12}N_1-(A_{21}+R_{21})N_2-2C_{up}N_2^2+W_{32}N_3+W_{ET}N_3N_{Ce}, \tag{2}$$

$$\frac{\mathrm{d}N_3}{\mathrm{d}t}=R_{13}N_1+C_{up}N_2^2-(W_{32}+R_{31})N_3-W_{ET}N_3N_{Ce}, \tag{3}$$

$$N_1+N_2+N_3=N_{Er}, \tag{4}$$

where N_1, N_2 and N_3 are Er^{3+} populations in energy levels $^4I_{15/2}$, $^4I_{13/2}$ and $^4I_{11/2}$, respectively. N_{Er} and N_{Ce} are the Er^{3+} and Ce^{3+} doped concentrations in the fiber core glass which are listed in Tab.1. R_{12} and R_{21} are the stimulated absorption and emission transition rates between $^4I_{15/2}$ and $^4I_{13/2}$ levels at signal wavelength, and R_{13} and R_{31} are the stimulated absorption and emission transition rates between $^4I_{15/2}$ and $^4I_{11/2}$ levels at 980 nm pump wavelength. A_{21} is the spontaneous radiative rate from $^4I_{13/2}$ level to $^4I_{15/2}$ level. C_{up} is the homogeneous up-conversion coefficient for the cross relaxation of $^4I_{13/2}+{}^4I_{13/2}\rightarrow{}^4I_{9/2}+{}^4I_{15/2}$. W_{32} is the multiphonon relaxation rate from $^4I_{11/2}$ level to $^4I_{13/2}$ level, and W_{ET} is the ET rate from Er^{3+}:$^4I_{11/2}$ level to Ce^{3+}:$^2F_{5/2}$ level.

The powers of signal light (P_s), pump light (P_p) and amplified spontaneous emission (ASE) noise light (P_{ASE}) propagating through the fiber are expressed as[14]

$$\frac{\mathrm{d}P_s}{\mathrm{d}z}=(\sigma_s^eN_2-\sigma_s^aN_1)P_s-\alpha_sP_s, \tag{5}$$

$$\frac{\mathrm{d}P_p^{\pm}}{\mathrm{d}z}=\pm(\sigma_p^eN_3-\sigma_p^aN_1)P_p^{\pm}\mp\alpha_pP_p^{\pm}, \tag{6}$$

$$\frac{\mathrm{d}P_{ASE}^{\pm}}{\mathrm{d}z}=\pm(\sigma_s^eN_2-\sigma_s^aN_1)P_{ASE}^{\pm}\pm$$

$$h\nu_{\mathrm{ASE}}\Delta\nu_{\mathrm{ASE}}\sigma_{\mathrm{s}}^{\mathrm{e}}N_2 \mp \alpha_{\mathrm{ASE}}P_{\mathrm{ASE}}^{\pm}, \quad (7)$$

where the subscripts s, p and ASE represent the signal, pump and ASE lights propagating forward (+) and backward (−), respectively. σ^{e}, σ^{a} and α denote the stimulated emission cross-section, absorption cross-section and fiber background loss, respectively. ν_{ASE} is the frequency of ASE noise, $\Delta\nu_{\mathrm{ASE}}$ is the effective bandwidth of ASE noise, and h is the Plank constant. Assuming a steady state condition, the set of differential equations is numerically integrated using the forth-order Runge-Kutta method with the known initial condition at the fiber input and output ends. The partial parameters needed for numerical calculations for Er^{3+} single-doped and Er^{3+}/Ce^{3+} co-doped glass samples are obtained from Refs.[2] and [15] and listed in Tab.2.

Tab.2 Parameters used for numerical simulations

Parameter	Symbol	Value for TEC2	Unit
Spontaneous emission rate of Er^{3+}	A_{21}	313.82	s^{-1}
Non-radiative transition rate of Er^{3+}	W_{32}	4 800	s^{-1}
Cooperative up-conversion coefficient	C_{up}	2.74×10^{-24}	$m^3\cdot s^{-1}$
Emission cross-section at 980 nm	$\sigma_{\mathrm{p}}^{\mathrm{e}}$	2.46×10^{-21}	cm^2
Absorption cross-section at 980 nm	$\sigma_{\mathrm{p}}^{\mathrm{e}}$	1.85×10^{-21}	cm^2
Er^{3+}-doped concentration	N_{Er}	3.78×10^{20}	cm^{-3}
Ce^{3+}-doped concentration	N_{Ce}	3.78×10^{20}	cm^{-3}
Er^{3+}-doped radius	r_{Er}	1.5	μm
Fiber core refractive index	n	2.019	−
Background loss	α	1.0	dB/m

The used 1.53 μm band stimulated absorption cross-section of Er^{3+} is determined from the measured absorption spectra based on the Beer-Lambert law, which can be expressed as[9]

$$\sigma_{\mathrm{a}}(\lambda) = 2.303\frac{OD(\lambda)}{N_{\mathrm{Er}}L}, \quad (8)$$

where N_{Er} is the Er^{3+} doped concentration, L is the sample thickness, and $OD(\lambda)$ is the absorption optical density. The used 1.53 μm band stimulated emission cross-section of Er^{3+} is calculated according to the McCumber theory, which can be expressed as[16]

$$\sigma_{\mathrm{e}}(\lambda) = \sigma_{\mathrm{a}}(\lambda)\exp[(\varepsilon - h\upsilon)/kT], \quad (9)$$

where k is the Boltzmann constant, and ε is the net free energy required to excite one Er^{3+} ion from $^4I_{15/2}$ level to $^4I_{13/2}$ level at temperature T.

Fig.5 shows the stimulated 1.53 μm band signal gain spectra of Er^{3+} single-doped and Er^{3+}/Ce^{3+} co-doped tellurite glass fibers based on TEC0 and TEC2 glass samples, respectively. The fiber with length of 50 cm is bi-directionally pumped at 980 nm with the power of 100 mW. The input signal is scanned from 1 520 nm to 1 620 nm with the power of −30 dBm. From Fig.5, it can be seen that the signal gain spectrum of 980 nm pumped tellurite glass fiber exhibits a broadband profile covering C-band and L-band regions, which is very favorable for the WDM communication system. Compared with the Er^{3+} single-doped TEC0 glass fiber, the signal gain in Er^{3+}/Ce^{3+} co-doped TEC2 glass fiber is increased over the entire spectrum, and an increment of about 2.4 dB and the maximum gain of 29.3 dB at signal wavelength of 1 532 nm are found.

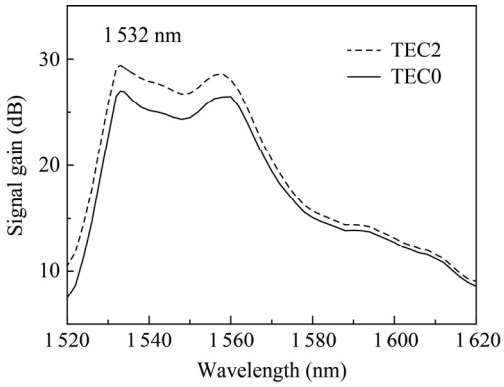

Fig.5 Simulated 1.53 μm signal gain spectra in the Er^{3+} single-doped and Er^{3+}/Ce^{3+} co-doped tellurite glass fibers under the 980 nm excitation

Er^{3+}/Ce^{3+} co-doped tellurite glasses with composition of TeO_2-GeO_2-Li_2O-Nb_2O_5 were prepared by conventional melt-quenching method. Er^{3+}/Ce^{3+} co-doping scheme can obviously improve the 1.53 μm band fluorescence emission of Er^{3+} through the ET from Er^{3+} to Ce^{3+} under the 980 nm excitation. Furthermore, the improved effect of Er^{3+}/Ce^{3+} co-doping on the 1.53 μm band signal gain is investigated, and the gain is improved by about 2.4 dB at 1 532 nm in the Er^{3+}/Ce^{3+} co-doped TEC2 glass fiber with length of 50 cm and pumping power of 100 mW at 980 nm. The results indicate that the Er^{3+}/Ce^{3+} co-doped tellurite glass has good prospect as a gain medium applied for 1.53 μm broadband and high-gain EDFAs.

References

[1] M. S. Sajna, Sunil Thomas, K. A. Ann Mary, Cyriac Joseph, P. R. Biju and N. V. Unnikrishnan, Journal of Luminescence **159**, 55 (2015).

[2] Y. Hu, S. Jiang, G. Sorbello, T. Luo, Y. Ding, B. C. Hwang and N. Peyghambarian, Journal of the Optical Society of America B-Optical Physics **18**, 1928 (2001).

[3] M. Çelikbilek, A. E. Ersundu, E.O. Zayim and S. Aydin, Journal of Alloys and Compounds **637**, 162 (2015).

[4] W. J. Zhang, J. Lin, M. Z. Cheng, S. Zhang, Y. J. Jia and J. H. Zhao, Journal of Quantitative Spectroscopy

and Radiative Transfer **159**, 39 (2015).
[5] R. Anthony, R. Lahiri and S. Biswas, Microwave and Optical Technology Letters **125**, 2463 (2014).
[6] A. Pandey, S. Som, V. Kumar, V. Kumar, K. Kumar, V. K. Rai and H. C. Swart, Sensors and Actuators B-Chemical **202**, 1305 (2014).
[7] S. C. Zheng, Y. W. Qi, S. X. Peng, D. D. Yin, Y. X. Zhou and S. X. Dai, Optoelectronics Letters **9**, 461 (2013).
[8] G. Dantelle, M. Mortier, D. Vivien and G. Patriarche, Optical Materials **28**, 638 (2006).
[9] T. Sasikala, L. R. Moorthy, K. Pavani and T. Chengaiah, Journal of Alloys and Compounds **542**, 271 (2012).
[10] B. R. Judd, Physical Review **127**, 750 (1992).
[11] G. S. Ofelt, Journal of Chemical Physics **37**, 511 (1962).
[12] M. R. Dousti, R. J. Amjad and Z. A. S. Mahraz, Journal of Molecular Structure **1079**, 347 (2015).
[13] P. Y. Wang, H. P. Xia, J. T. Peng, H. Y. Hu, L. Tang, Y. P. Zhang, B. J. Chen and H. J. Jiang, Optoelectronics Letters **9**, 285 (2013).
[14] G. R. Khan, Optical Fiber Technology **18**, 421 (2012).
[15] Y. X. Zhou, D. D. Yin, S. C. Zheng and X. C. Xu, Journal of Quantitative Spectroscopy and Radiative Transfer **129**, 1 (2013).
[16] D. E. McCumber, Physical Review **136**, 954 (1964).